♦ A Bio-Inspired Approach to Controlled Crystallization at the Nanoscale

Joanna Aizenberg

Nature produces a wide variety of exquisite mineralized tissues fulfilling diverse functions, often from simple inorganic salts. Organisms exercise a level of molecular control over the physico-chemical properties of inorganic crystals that is unparalleled in today's technology. This reflects directly or indirectly the controlling activity of biological organic surfaces that are involved in the formation of these materials. Biological materials are intrinsically nanoscale. Biomineralization occurs within specific nanoenvironments, which implies stimulation of crystal formation at certain interfacial sites and relative inhibition of the process at all other sites. Our approach to artificial crystallization is based on the combination of the two latter concepts—i.e., the use of organized organic surfaces patterned with specific initiation domains on a nanoscale to study and orchestrate the crystallization process. This bio-inspired engineering effort made it possible to achieve a remarkable level of control over various aspects of the crystal nucleation and growth, including the precise localization of particles, nucleation density, crystal sizes, morphology, crystallographic orientation, arbitrary shapes, nanostructure, stability, and architecture. The ability to construct large, defect-free, patterned single crystals with controlled nanoporosity; periodic arrays of uniform, oriented nanocrystals; or films presenting patterns of nanocrystals offers a new, bio-inspired nanotechnology route to materials engineering. © 2005 Lucent Technologies Inc.

Introduction

Crystallization is a key process in the synthesis of many technologically important materials [25, 41, 43, 45, 51]. Our knowledge of basic crystallization mechanisms—e.g., what defines the location and density of nucleation, polymorph selectivity, or face-selective nucleation and, after the specific nucleus is formed, what determines crystal sizes, shapes, and architecture of the formed crystals and their stability—is, however, extremely limited. Better understanding of these processes is essential in engineering advanced materials with controlled properties.

In contrast, the formation of crystalline materials in nature is highly regulated [36, 37, 42]. Different organisms, irrespective of their systematic position, exercise a level of molecular control over the physico-chemical properties of minerals that is almost

unthinkable in artificial processes. It is achieved by means of organized assemblies of specialized biological macromolecules. Recently, new synthetic strategies that mimic biomineralization have been developed [1, 2, 7, 11, 31, 32, 38, 39]. These promising approaches utilize processes involving molecular recognition at the organic-inorganic interfaces. A number of elegant studies demonstrate the use of simplified molecular assemblies that resemble biological membranes, such as Langmuir monolayers [17, 22, 26, 31, 32, 40, 50], self-assembled monolayers (SAMs) [13, 15, 20, 21, 23], biological macromolecules [1, 2, 11], and surfactant aggregates [8, 18, 48], as the nucleation templates. Most of these studies, however, address only one "crystallization problem" at a time—e.g, oriented nucleation, polymorph specificity, or shapes of the growing crystals.

This paper describes our approach to govern crystallization [3, 4] based on engineering the nucleation site and on controlling mass transport to the surface at the micron scale, using micropatterned SAMs of alkanethiols supported on metal films. This method, which we apply to crystallization of calcium carbonate, makes it possible, for the first time, to achieve nanoscale control over many of the crucial aspects of nucleation and crystal growth—oriented nucleation, location and density of nucleation, crystal sizes and patterns—in one experiment.

Experimental

The materials, experimental setup and characterization techniques used in this study are described below.

Substrates

Silicon wafers were coated with 2 nm of Ti, to promote adhesion, and then with 50 nm of metal (Ag or Au) using an electron beam evaporator.
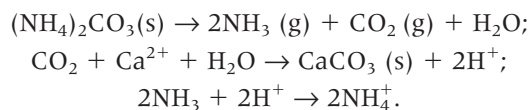
SAMs

SAMs of $HS(CH_2)_{15}CO_2H$, $HS(CH_2)_{11}OH$, $HS(CH_2)_{11}SO_3H$, $HS(CH_2)_{11}PO_3H_2$, $HS(CH_2)_{15}CH_3$, $HS(CH_2)_{11}N(CH_3)_3Cl$ were formed on metal substrates by exposing the surfaces to a 10 mM solution of the thiol in ethanol for 24 h, followed by washing with ethanol [33]. Patterned SAMs were formed using microcontact printing (μCP) [27, 28]: elastomeric stamps with different relief structures were "inked" with a 10 mM

solution of $HS(CH_2)_nX$ in ethanol and brought into conformal contact with gold for 10 s; the non-contact areas were then derivatized with a 10 mM solution of $HS(CH_2)_nY$ in ethanol by immersion for 1 min.

Crystallization

The substrates were placed upside down (to ensure that only particles grown on the SAM would be bound to the surface) in 10 mM calcium chloride solution in a closed desiccator containing vials of ammonium carbonate [1, 3, 4, 6, 12]. All experiments were carried out at room temperature for 1 h. Precipitation of calcium carbonate resulted from the diffusion of carbon dioxide vapor into the $CaCl_2$ solution, according to the following reactions:

$$(NH_4)_2CO_3(s) \rightarrow 2NH_3\ (g) + CO_2\ (g) + H_2O;$$
$$CO_2 + Ca^{2+} + H_2O \rightarrow CaCO_3\ (s) + 2H^+;$$
$$2NH_3 + 2H^+ \rightarrow 2NH_4^+.$$

Analysis

The crystals, once formed, were examined using optical microscopy to determine the densities of nucleation and crystal sizes. The specific crystallographic orientations of the crystals relative to the interface between the SAM and the solution were analyzed using XRD in the θ–2θ scan mode. A detailed morphological analysis was undertaken to confirm the assignment of each specific crystallographic orientation and to estimate the deviation in angle of the crystals from these directions of growth.
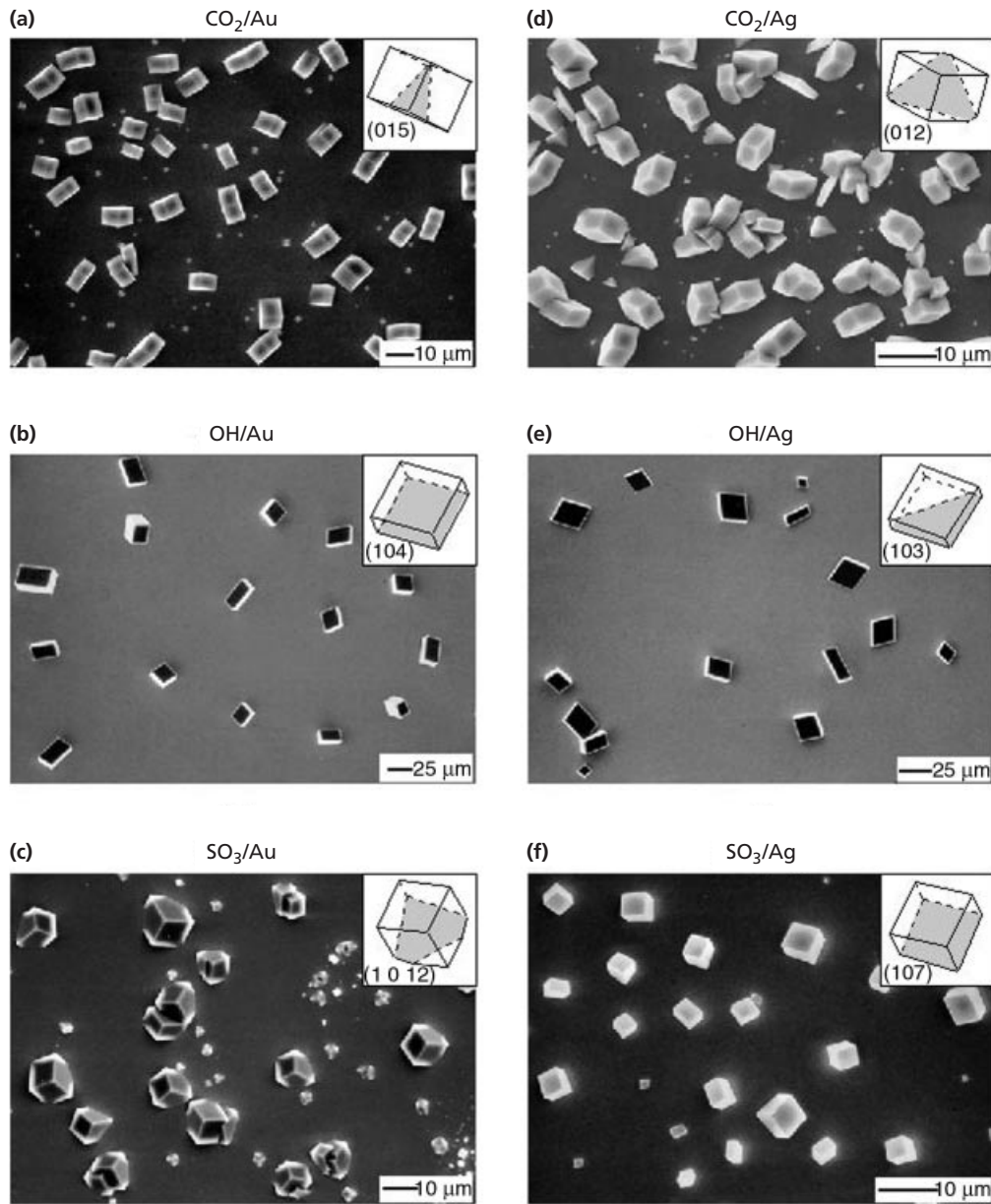
Results and Discussion

The results of our study describing the two important aspects of crystal engineering at the nanoscale—how to control the oriented nucleation and patterned crystal growth—are discussed below.

Oriented Nucleation

We chose the crystallization of calcite on SAMs of alkanethiols $HS(CH_2)_nX$ bearing negatively charged headgroups (X = CO_2^-, SO_3^-, OH) as a model system for three reasons (**Figure 1**):

- Calcite has a simple structure, and its crystallization is relatively easy to perform (there is extensive background information describing this process [1, 9, 11–13, 17, 19, 36, 40, 46]).

(a) CO_2/Au — (015)

(d) CO_2/Ag — (012)

(b) OH/Au — (104)

(e) OH/Ag — (103)

(c) SO_3/Au — (1 0 12)

(f) SO_3/Ag — (107)

The inserts present computer-generated simulations of the regular calcite rhombohedra viewed down perpendicular to the corresponding average nucleating face (shadowed).

Figure 1.
Scanning electron micrographs showing the face-selective nucleation of calcite crystals mediated by SAMs.

- Formation of crystallographically oriented, exquisitely shaped calcite crystals with unique materials properties is common in biological environments [37, 42] and is believed to be controlled by acidic macromolecules, conceivably by virtue of a match between the structure of the organic surface and that of a particular crystal plane [1, 2, 6, 12].

- Alkanethiols self-assemble on metal substrates into highly ordered, crystalline monolayers with various structural parameters [16, 29, 30, 44, 47] and present, therefore, an attractive candidate for

an organized organic surface to mediate crystallization [3, 4, 13, 15, 20, 21, 23].

Alkanethiols terminated in different functional groups assemble on Au(111) in a hexagonal overlayer characterized by the interchain distance $a = 4.97$ Å, the tilt of the chain $\alpha = 28$–$32°$ and the twist angle around the axis of the chain $\beta = 50$–$55°$ [44]. On Ag(111), X-terminated alkanethiols self-assemble in a hexagonal array with $a = 4.77$ Å, $\alpha = 8$–$12°$, $\beta = 42$–$45°$ [30]. The presence of counterions, such as Cd^{2+} and Ca^{2+}, has been shown to induce an additional ordering of terminal acidic headgroups in SAMs [4, 14, 34, 35, 49]. We anticipated that different SAMs—those terminated in different functional groups and even those bearing the same terminal group but supported on different metals—would induce oriented nucleation of calcite in different crystallographic directions. Indeed, crystallization experiments with CO_2^-, SO_3^- and OH-terminated SAMs supported on Au and Ag produced arrays of highly oriented calcite crystals [4], nucleated from crystallographic planes specific to each surface type (see Figure 1).

The predominant nucleating planes (NP) of the calcite crystals were first determined from the XRD profiles [4]. To confirm the assignment of each specific crystallographic orientation and to estimate the angular deviation from these directions of growth, a detailed morphological analysis was performed. For each surface type, a population of 40 crystals was used in statistics. The crystals were viewed down the surface normal in a scanning electron microscope. We measured the angles between the crystal edges meeting at the upper corner of the crystal. These angles can be unequivocally related to the orientation of the regular (104) calcite rhombohedra vis-à-vis the interface, using structural relationships in the calcite unit cell [9, 36]. The morphological results were visualized using the sphere of reflection (**Figure 2**, top).

The nucleating planes for each surface type were plotted as circles on the sphere with a 5% gray scale; the intensity of the gray scale of the final circles is proportional to the number of crystals in the corresponding orientation [4]. The example shown in Figure 2 (top) corresponds to the morphological measurements of a set of 40 crystals in which one crystal nucleated from the (101) plane, two from the (110), three from the (100), four from the (113), five from the (104), six from the (012), eight from the (018), and 11 from the (001) plane. A significant clustering of the data was observed for each surface type, indicative of a high degree of orientational specificity induced by SAMs. The positions of the average nucleating planes estimated from the morphological analysis (NP$_{MA}$) were compared to the predominant orientations observed in the corresponding X-ray diffraction profiles (NP$_{XRD}$) (indicated by arrows).

Table I summarizes the results of oriented crystal growth on CO_2^-, SO_3^- and OH-terminated SAMs supported on Au and Ag.

We believe that the orientational uniformity of crystals formed on each surface is controlled by the specific interfacial structure of the oriented, homogeneous SAM. It is noteworthy that for each pair X/Au and X/Ag, the difference in crystallographic orientations of calcite crystals ($\sim$15–20°) corresponds to the difference in the tilt of the alkanethiol molecules in the SAMs on Au and Ag. This relationship is illustrated in **Figure 3**, which presents the example of oriented nucleation of calcite from the (015) and (012) crystallographic planes induced by SAMs of $HS(CH_2)_{15}CO_2H$/Au and $HS(CH_2)_{15}CO2H$/Ag. It is also important to note that, in most cases, we did not observe a satisfactory match between the lattices of the SAMs and the crystal planes they nucleate. On the other hand, there always existed a certain orientation of the functional groups in the SAM that precisely matched the orientation of the carbonate ions in the nucleated crystal (Figure 3). Careful study of this relationship showed that the orientation of inorganic crystals at the organic interface is governed by the orientation of the functional groups [5, 24].

Patterned Crystal Growth

Another important advantage of using SAMs of alkanethiols as nucleation templates compared to other supramolecular assemblies is that they can be easily patterned on a micron scale [27, 28]. We used this property to control area-selective crystallization.
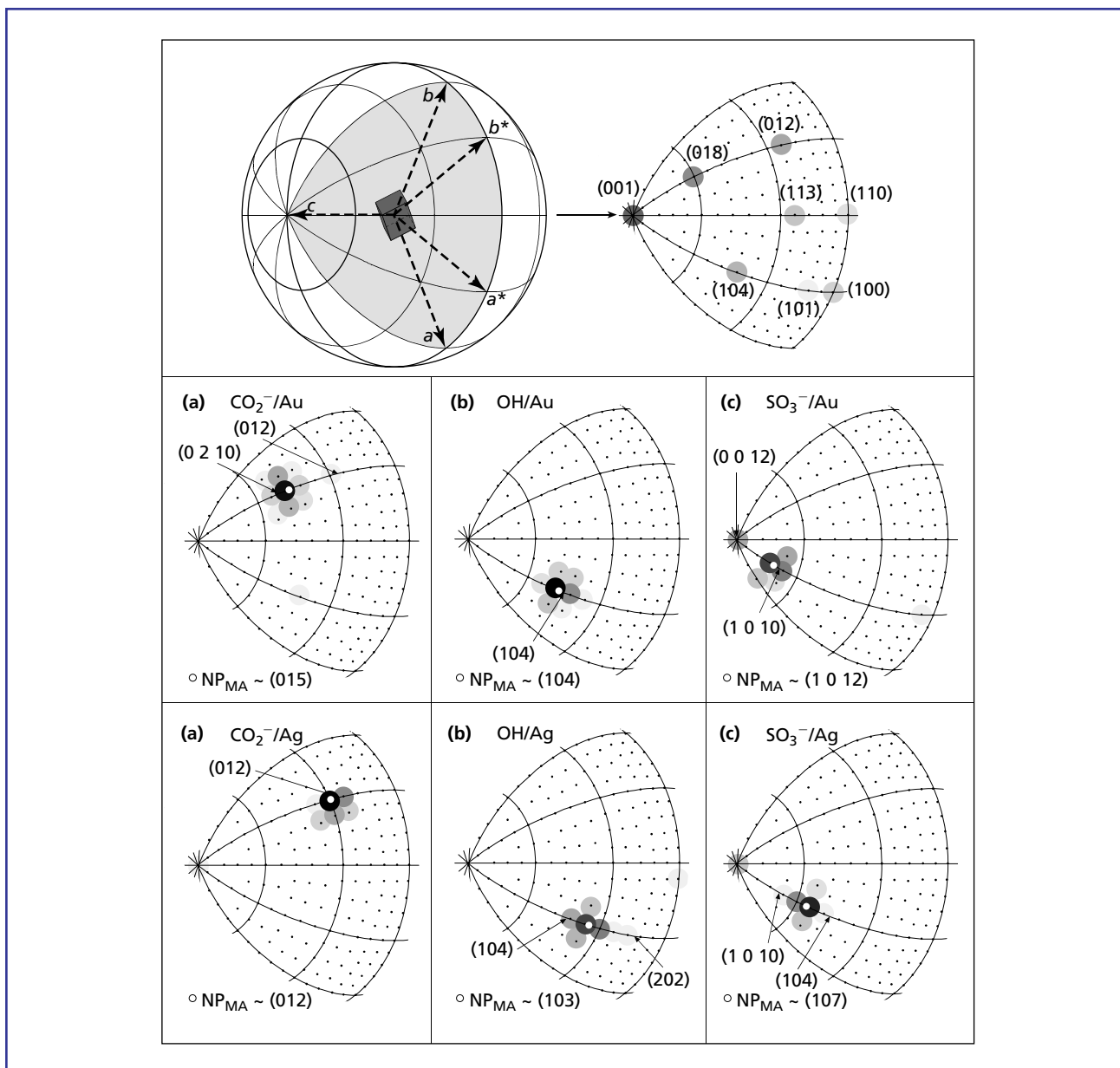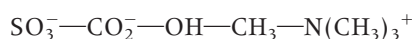
Figure 2.
Pole figure presentation of morphological data for the orientations of calcite crystal grown on different SAMs.

The analysis of the nucleation activity of various SAMs showed the induction time of calcite nucleation to increase and the density of nucleation to decrease in the following sequence:

$$SO_3^- — CO_2^- — OH — CH_3 — N(CH_3)_3^+$$

Patterned SAMs of ω-terminated alkanethiols (see **Figure 4**) with a controlled distribution of more active nucleation sites within a less active background were formed by μCP (Figure 4a). Crystallization of calcite on these substrates resulted in the formation of large-area, high-resolution inorganic replicas of the underlying organic patterns [3]. The observed patterned crystallization can be explained in terms of diffusion-limited, island-specific nucleation [3, 10]. Figure 4b describes the mechanism of the process. After the nucleation begins at rapidly nucleating SAMs, the ion flux into these regions depletes calcium carbonate

Table I. Average nucleation plane and percentage of oriented calcite crystals grown on SAMs supported on gold and silver.

SAM	Au					Ag				
	Nucleation plane, NP_{MA}*	Dihedral angle, δ†	Angular deviation‡	Percentage of oriented crystals		Nucleation plane, NP_{MA}*	Dihedral angle, δ†	Angular deviation‡	Percentage of oriented crystals	
				From morphological analysis	From XRD analysis				From morphological analysis	From XRD analysis
CO_2^-	(015)	41°	4.3°	97	73	(012)	60°	3.6°	97	82
OH	(104)	43°	3.6°	100	91	(103)	56°	5.1°	97	81
SO_3^-	(1 0 12)	21°	3.4°	78	56	(107)	35°	2.7°	78	63

*Average nucleation plane NP_{MA} corresponds to the highest density in Figure 2 (open circles).
†Average dihedral angle between the NP_{MA} and (001) plane.
‡Standard angular deviation from the NP_{MA}.

HS(CH₂)₁₅CO₂H/Au

Surface normal · *c*-axis

$\delta = 41°$

$\Delta\delta \cong \Delta\alpha$

(015)

$\alpha = 28–32°$

Au

HS(CH₂)₁₅CO₂H/Ag

Surface normal · *c*-axis

$\delta = 60°$

(012)

$\alpha = 8–12°$

Ag

(a) Relative orientations of the SAM and nucleated crystals. Note the possible co-alignment of the CO_2 groups in the SAM and of the carbonates in the nucleated face.

(b) Mismatch between the lattices of the CO_2 groups in the undistorted SAM (large open circles) and the Ca ions in the nucleated face (small solid circles).
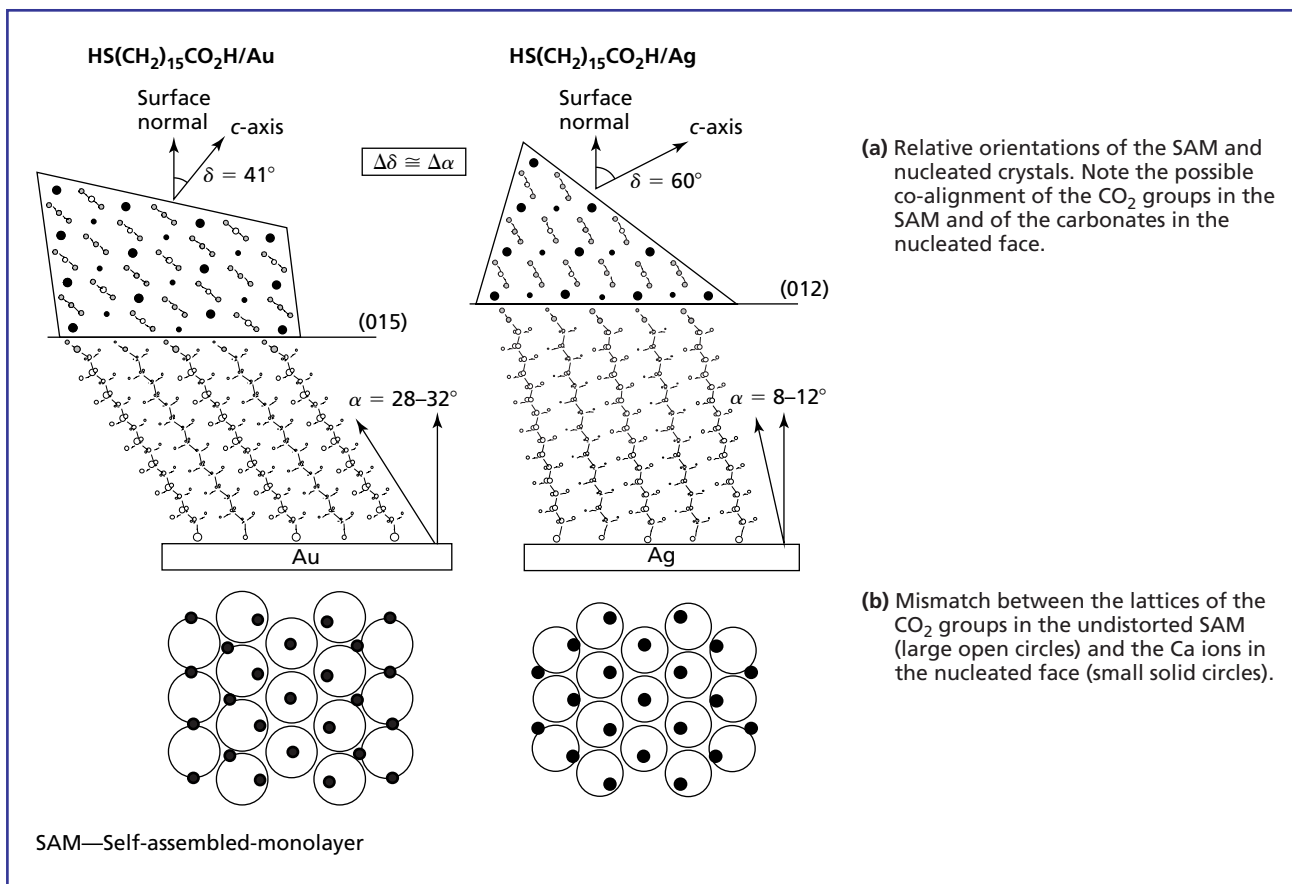
SAM—Self-assembled-monolayer

Figure 3.
Schematic presentation (to scale) of the geometrical relationship between the structure of the SAMs of HS(CH₂)₁₅ CO₂H supported on gold (left) and silver (right) and the oriented calcite crystal they nucleate.

concentration over slowly nucleating zones. In the region l_d where the effective concentration of the solution is below saturation (c_{sat}), nucleation does not occur. Nucleation on slowly nucleating regions is allowed only for distances from the rapidly nucleating region $x > l_d$, where $c > c_{sat}$. This mechanism was confirmed in the experiment, in which calcite crystals were grown on a methyl-terminated surface with one isolated carboxylic acid terminated region: the halo pattern clearly seen in the scanning electron micrograph (Figure 4b) corresponds to the depletion region l_d. Therefore, if we keep the distance between rapidly nucleating regions below $2l_d$, crystallization will be entirely restricted to the rapidly nucleating regions (Figure 4b).

By adjusting various parameters of our experimental setup (concentration of the crystallizing solution, density and sizes of features in the stamp, and functionality of the surface of the SAM), we can exert further control over the crystallization process: in addition to precise localization of nucleation, we can define the density of the active nucleating regions on the surface (N) and the number of crystals that nucleate within each region (n), as well as their crystallographic orientation. **Figure 5** presents a set of patterns of calcite crystals that exemplify the general algorithm that we used to control crystallization:

- We chose a specific X-terminated alkanethiol/ metal combination to induce the desired oriented crystallization.
- For a given *N*, we determined the corresponding distance between the features in the stamp: $p = N^{-1/2}$.
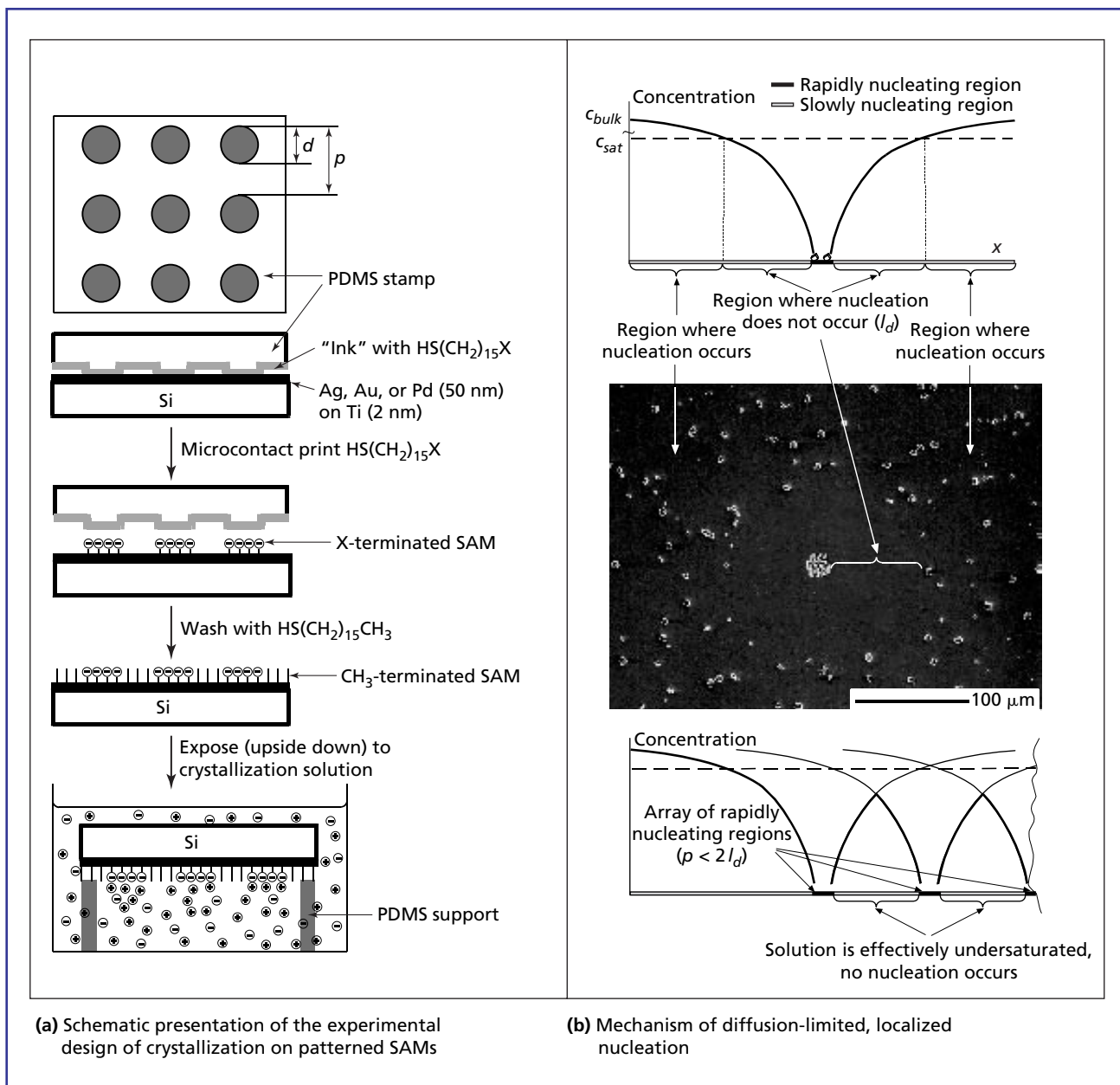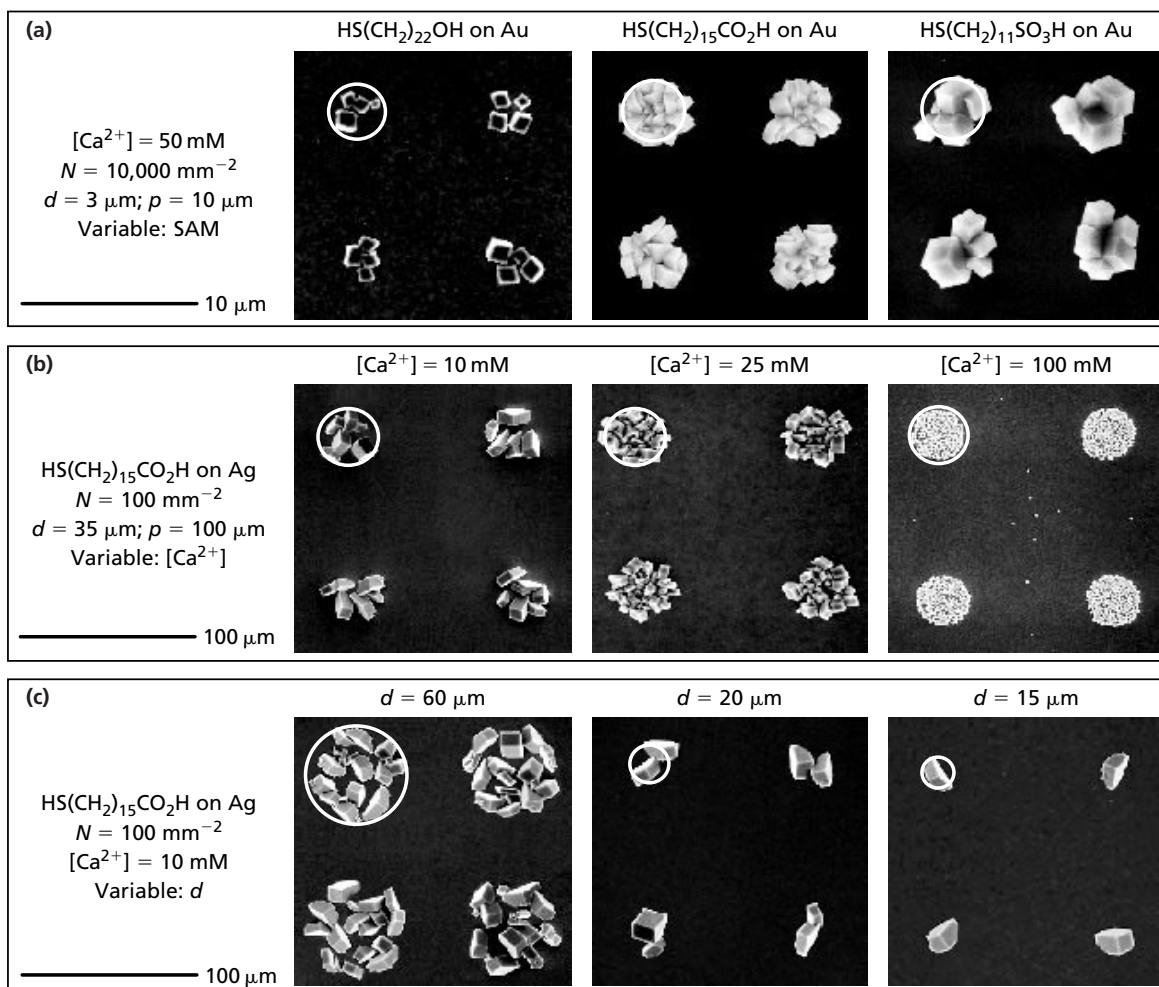
(a) Schematic presentation of the experimental design of crystallization on patterned SAMs

(b) Mechanism of diffusion-limited, localized nucleation

Figure 4.
Experimental approach to nanopatterned crystallization.

- By varying the concentration of the crystallizing solution, we defined the range of concentrations for which $l_d > p/2$, so that inhibition of nucleation occurs over the entire slowly nucleating regions due to the mass transport to the regions of crystal growth. For example, for patterned crytallization on a SAM supported on Ag and consisting of circles of $HS(CH_2)_{15}CO_2H$

($d = 35$ μm, $p = 100$ μm) in the field of $HS(CH_2)_{15}CH_3$, the required concentrations for the $CaCl_2$ solution are below 100 mM (for higher concentrations, sporadic formation of crystals on the CH_3-terminated regions remote from the CO_2H-terminated sites occurred).

- At constant concentration, the number of crystals, n, within each active nucleation region appears

Figure 5.
Control over nucleation of calcite by micropatterned SAMs consisting of a square array of rapidly nucleating circles—SAMs of HS(CH$_2$)$_n$X—in a slowly nucleating background—SAMs of HS(CH$_2$)$_{15}$CH$_3$.

(a) HS(CH$_2$)$_{22}$OH on Au · HS(CH$_2$)$_{15}$CO$_2$H on Au · HS(CH$_2$)$_{11}$SO$_3$H on Au

[Ca^{2+}] = 50 mM
N = 10,000 mm^{-2}
d = 3 μm; p = 10 μm
Variable: SAM

——— 10 μm

(b) [Ca^{2+}] = 10 mM · [Ca^{2+}] = 25 mM · [Ca^{2+}] = 100 mM

HS(CH$_2$)$_{15}$CO$_2$H on Ag
N = 100 mm^{-2}
d = 35 μm; p = 100 μm
Variable: [Ca^{2+}]

——— 100 μm

(c) d = 60 μm · d = 20 μm · d = 15 μm

HS(CH$_2$)$_{15}$CO$_2$H on Ag
N = 100 mm^{-2}
[Ca^{2+}] = 10 mM
Variable: d

——— 100 μm

SAM—Self-assembled monolayer

The overlaid circles outline the geometry of the pattern. The experimental parameters—density (N) and sized (d) of features in the stamp, concentration of the crystallizing solution, functionality of the surface of the SAM, and a supporting metal—are indicated.
(a) Patterned oriented crystallization induced by SAMs terminated in different functional groups.
(b) Nucleation density and extent of area-selective nucleation on SAMs of HS(CH$_2$)$_{15}$CO$_2$H supported on Ag as a function of concentration of crystallizing solution for a given distribution and size of the rapidly nucleating regions [d = 35 μm, p = 100 μm]. The increase in concentration results in occasional crystallization on the methyl-terminated region, in agreement with the expected decrease in the size of the zone l_d.
(c) Number of crystals per active nucleation region (n) as a function of its area.

to depend linearly upon its area [3]. This relation made it possible to determine the optimum size, *d*, of the raised features in the stamp for any chosen *n*.

Using this algorithm, we were able to determine the necessary experimental conditions—concentration of the crystallizing solution, geometric characteristics and functionality of the micropatterned SAM, supporting
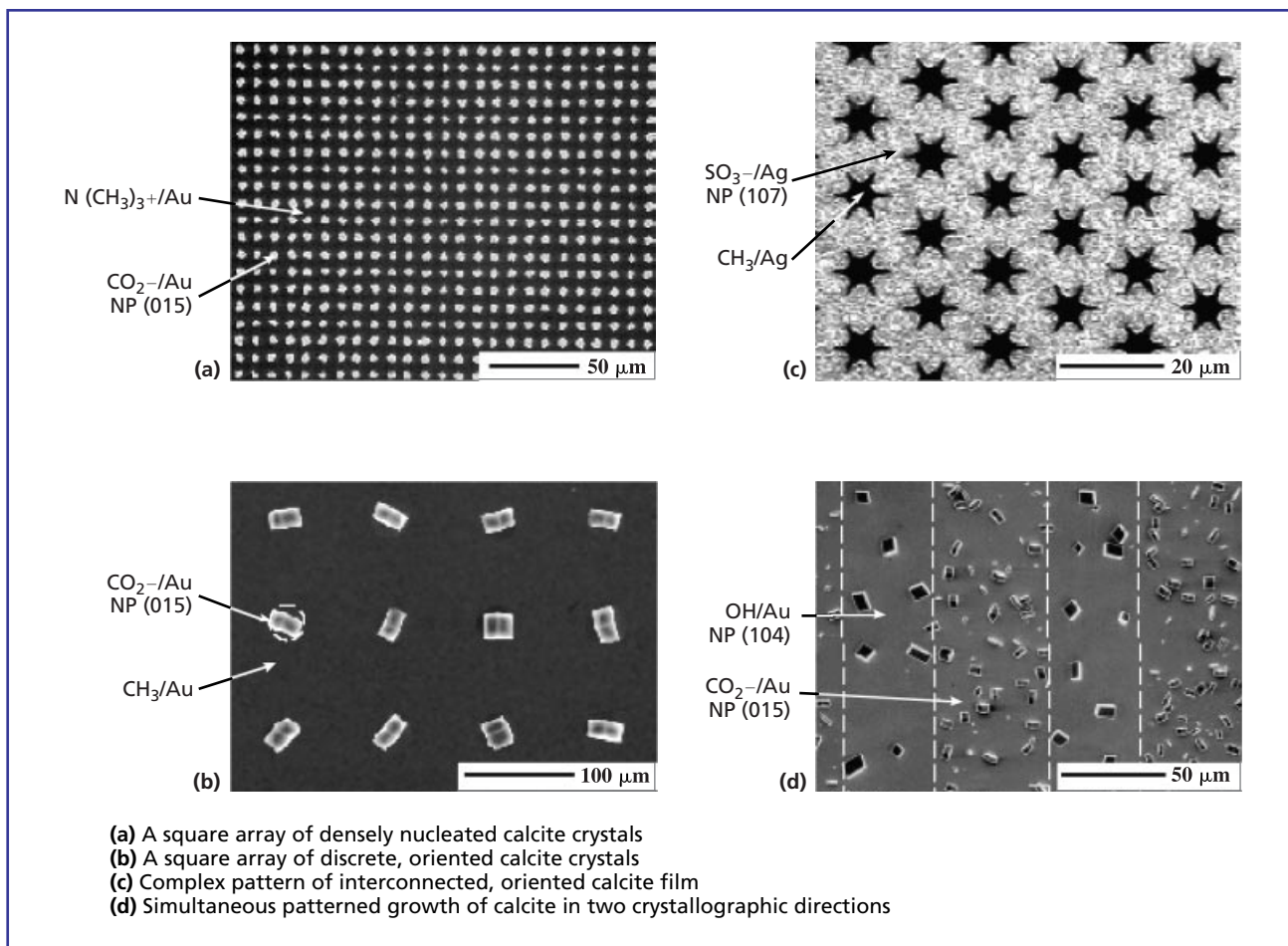
(a) A square array of densely nucleated calcite crystals
(b) A square array of discrete, oriented calcite crystals
(c) Complex pattern of interconnected, oriented calcite film
(d) Simultaneous patterned growth of calcite in two crystallographic directions

Figure 6.
Scanning electron micrographs showing the controlled crystallization of calcite on patterned SAMs.

metal—to fabricate arbitrary nanopatterns of oriented calcite nanocrystals (**Figure 6**). The crystals can be grown in dense, oriented islands (Figure 6a) or in highly ordered two-dimensional arrays of single calcite crystals of uniform size and orientation (Figure 6b); we can reverse the crystallization pattern and fabricate interconnected, oriented films of calcite crystals with the edge resolution of <50 nm (Figure 6c); patterned growth of calcite in different crystallographic directions can be achieved by using substrates patterned with SAMs that have similar nucleating activity but induce nucleation from different crystallographic planes (Figure 6d).

Conclusions

Diffusion-controlled growth of calcite in nature is a well-known phenomenon [36, 37, 42]. Formation of intricate biogenic calcitic structures usually occurs from organized macromolecules in specific micro-environments that provide the directional flux of ions toward the growing crystals [37, 42]. The power of the presented bio-inspired approach to artificial crystallization is, therefore, based on our ability to govern mass transport to different regions of the surface at a micron scale and to control the molecular structure and nanoenvironment of the nucleation site, by patterning ω-terminated SAMs into regions with different nucleating activity. Using crystallization of calcite as an example, we demonstrate that we can regulate the precise location, density and area of the regions active for nucleation, and thereby the number, size, and crystallographic orientation of the crystals that nucleate in each part of the surface.

We conclude, therefore, that the combination of three major ideas—(1) the ability of SAMs to nucleate

growth from a single crystallographic plane, (2) patterning SAMs with nano/micro-regions having different nucleating activity, and (3) taking advantage of mass transport and the proper size of the nanopattern, so that the ion flux into the regions of crystal growth keeps the concentration of the crystallizing solution over slowly nucleating regions low enough that nucleation effectively never happens—provides a simple and convenient route to control nucleation. We believe that this method could find applications in engineering of oriented inorganic nanomaterials with complex form, such as ceramics or semiconductors whose mechanical, optical, and electrical performance can be regulated by controlling the sizes, distribution, crystallographic orientation, and morphology of the constituent crystals.

References

[1] L. Addadi, J. Moradian, E. Shay, N. G. Maroudas, and S. Weiner, "A Chemical Model for the Cooperation of Sulfates and Carboxylates in Calcite Crystal Nucleation: Relevance to Biomineralization,". Proc. Nat. Acad. Sci., 84 (1987), 2732–2736.

[2] L. Addadi and S. Weiner, "Interactions Between Acidic Proteins and Crystals: Stereochemical Requirements in Biomineralization," Proc. Nat. Acad. Sci., 82 (1985), 4110–4114.

[3] J. Aizenberg, A. J. Black, and G. M. Whitesides, "Control of Nucleation by Patterned Self-Assembled Monolayers," Nature, 398:6727 (1999), 495–498.

[4] J. Aizenberg, A. J. Black, and G. M. Whitesides, "Oriented Growth of Calcite Controlled by Self-Assembled Monolayers of Functionalized Alkanethiols Supported on Gold and Silver," J. Am. Chem. Soc., 121:18 (1999), 4500–4509.

[5] J. Aizenberg, D. A. Muller, J. L. Grazul, and D. R. Hamann, "Direct Fabrication of Large Micropatterned Single Crystals," Science 299:5610 (2003), 1205–1208.

[6] S. Albeck, J. Aizenberg, L. Addadi, and S. Weiner, "Interactions of Various Skeletal Intracrystalline Components with Calcite Crystals," J. Am. Chem. Soc., 115:25 (1993), 11691–11697.

[7] M. Alper, P. D. Calvert, R. Frankel, P. C. Rieke, and D. A. Tirrell (eds.), Materials Synthesis Based on Biological Processes, Mat. Res. Soc., Pittsburgh, PA, 1991.

[8] D. D. Archibald and S. Mann, "Template Mineralization of Self-Assembled Anisotropic Lipid Microstructures," Nature, 364:6436 (1993), 430–433.

[9] D. D. Archibald, S. B. Qadri, and B. P. Gaber, "Modified Calcite Deposition due to Ultrathin Organic Films on Silicon Substrate," Langmuir, 12:2 (1996), 538–546.

[10] A.-L. Barabási and H. E. Stanley, Fractal Concepts in Surface Growth, Cambridge Univ. Press, New York, NY, 1995.

[11] A. M. Belcher, R. J. Christensen, P. K. Hansma, G. D. Stucky, and D. E. Morse, "Control of Crystal Phase Switching and Orientation by Soluble Mollusc-Shell Proteins," Nature, 381:6577 (1996), 56–58.

[12] A. Berman, L. Addadi, and S. Weiner, "Interactions of Sea-Urchin Skeleton Macromolecules with Growing Calcite Crystals—A Study of Intracrystalline Proteins," Nature, 331 (1988), 546–548.

[13] A. Berman, D. J. Ahn, A. Lio, M. Salmeron, A. Reichert, and D. Charych, "Total Alignment of Calcite at Acidic Polydiacetylene Films—Cooperativity at the Organic-Inorganic Interface," Science, 269:5223 (1995), 515–518.

[14] C. Böhm, F. Leveiller, D. Jacquemain, H. Mohwald, K. Kjaer, J. Alsnielsen, I. Weissbuch, and L. Leiserowitz, "Packing Characteristics of Crystalline Monolayers of Fatty-Acid Salts, at the Air Solution Interface, Studied by Grazing-Incidence X-Ray Diffraction," Langmuir, 10:3 (1994), 830–836.

[15] B. C. Bunker, P. C. Rieke, B. J. Tarasevich, A. A. Campbell, G. E. Fryxell, G. L. Graff, L. Song, J. Liu, J. W. Virden, and G. L. McVay, "Ceramic Thin-Film Formation on Functionalized Interfaces Through Biomimetic Processing," Science, 264: 5155 (1994), 48–55.

[16] N. Camillone, C. E. D. Chidsey, G. Liu, and G. Scoles, "Superlattice Structure at the Surface of a Monolayer of Octadecanethiol Self-Assembled on Au(111)," J. Chem. Phys., 98:4 (1993), 3503–3511.

[17] P. W. Carter and M. D. Ward, "Topographically Directed Nucleation of Organic-Crystals on Molecular Single-Crystal Substrates," J. Am. Chem. Soc., 115: 24 (1993), 11521–11535.

[18] T. Douglas, D. P. E. Dickson, S. Betteridge, J. Charnock, C. D. Garner and S. Mann, "Synthesis and Structure of an Iron(Iii) Sulfide-Ferritin Bioinorganic Nanocomposite," Science, 269:5220 (1995), 54–57.

[19] G. Falini, S. Albeck, S. Weiner, and L. Addadi, "Control of Aragonite or Calcite Polymorphism

by Mollusk Shell Macromolecules," Science, 271:5245 (1996), 67–69.

[20] S. Feng and T. Bein, "Growth of Oriented Molecular-Sieve Crystals on Organophosphonate Films," Nature, 368: 6474 (1994), 834–836.

[21] L. M. Frostman, M. M. Bader, and M. D. Ward, "Nucleation and Growth of Molecular-Crystals on Self-Assembled Monolayers," Langmuir, 10: 2 (1994), 576–582.

[22] L. M. Frostman and M. D. Ward, "Nucleation of Molecular Crystals Beneath Guanidinium Alkanesulfonate Monolayers," Langmuir, 13:2 (1997), 330–337.

[23] V. K. Gupta and N. L. Abbott, "Design of Surfaces for Patterned Alignment of Liquid Crystals on Planar and Curved Substrates," Science, 276:5318 (1997), 1533–1536.

[24] Y.-J. Han and J. Aizenberg, "Face-Selective Nucleation of Calcite on Self-Assembled Monolayers of Alkanethiols: Effect of the Parity of the Alkyl Chain," Angew. Chem. Int. Ed. 42 (2003), 3668–3670.

[25] A. H. Heuer, D. J. Fink, V. J. Laraia, J. L. Arias, P. D. Calvert, K. Kendall, G. L. Messing, J. Blackwell, P. C. Rieke, D. H. Thompson, A. P. Wheeler, A. Veis, and A. I. Caplan, "Innovative Materials Processing Strategies—A Biomimetic Approach," Science, 255:5048 (1992), 1098–1105.

[26] B. R. Heywood and S. Mann, "Organic Template-Directed Inorganic Crystallization— Oriented Nucleation of Baso4 Under Compressed Langmuir Monolayers," J. Am. Chem. Soc., 114: 12 (1992), 4681–4686.

[27] A. Kumar, N. A. Abbott, E. Kim, H. A. Biebuyck, and G. M. Whitesides, "Patterned Self-Assembled Monolayers and Meso-Scale Phenomena," Acc. Chem. Res., 28 (1995), 219–226.

[28] A. Kumar, H. A. Biebuyck, and G. M. Whitesides, "Patterning Self-Assembled Monolayers—Applications in Materials Science," Langmuir, 10:5 (1994), 1498–1511.

[29] P. E. Laibinis and G. M. Whitesides, "Self-Assembled Monolayers of N-Alkanethiolates on Copper Are Barrier Films That Protect the Metal Against Oxidation by Air," J. Am. Chem. Soc., 114:23 (1992), 9022–9028.

[30] P. E. Laibinis, G. M. Whitesides, D. L. Allara, Y. T. Tao, A. N. Parikh, and R. G. Nuzzo, "Comparison of the Structures and Wetting Properties of Self- Assembled Monolayers of Normal-Alkanethiols on the Coinage Metal-Surfaces, Cu, Ag, Au," J. Am. Chem. Soc., 113:19 (1991), 7152–7167.

[31] E. M. Landau, M. Levanon, L. Leiserowitz, M. Lahav, and J. Sagiv, "Transfer of Structural Information from Langmuir Monolayers to Three-Dimensional Growing Crystals," Nature, 318 (1985), 353–356.

[32] E. M. Landau, S. G. Wolf, M. Levanon, L. Leiserowitz, M. Lahav, and J. Sagiv, "Stereochemical Studies in Crystal Nucleation. Oriented Crystal Growth of Glycine at Interfaces Covered with Langmuir and Langmuir-Blodgett Films of Resolved a-Amino Acids," J. Am. Chem. Soc., 111 (1989), 1436–1445.

[33] N. B. Larsen, H. Biebuyck, E. Delamarche, and B. Michel, "Order in Microcontact Printed Self-Assembled Monolayers," J. Am. Chem. Soc., 119:13 (1997), 3017–3026.

[34] F. Leveiller, D. Jacquemain, M. Lahav, L. Leiserowitz, M. Deutsch, K. Kjaer, and J. Alsnielsen, "Crystallinity of the Double-Layer of Cadmium Arachidate Films at the Water-Surface," Science, 252:5012 (1991), 1532–1536.

[35] J. Li, K. S. Liang, G. Scoles, and A. Ulman, "Counterion Overlayers at the Interface Between an Electrolyte and an Omega-Functionalized Monolayer Self-Assembled on Gold—An X-Ray Reflectivity Study," Langmuir, 11:11 (1995), 4418–4427.

[36] F. Lippmann, Sedimentary Carbonate Minerals, Springer-Verlag, Berlin, Ger., 1973.

[37] H. A. Lowenstam and S. Weiner, On Biomineralization, Oxford Univ. Press, New York, NY, 1989.

[38] S. Mann, "Molecular Tectonics in Biomineralization and Biomimetic Materials Chemistry," Nature, 365:6446, (1993), 499–505.

[39] S. Mann, D. D. Archibald, J. M. Didymus, T. Douglas, B. R. Heywood, F. C. Meldrum, and N. J. Reeves, "Crystallization at Inorganic-Organic Interfaces—Biominerals and Biomimetic Synthesis," Science, 261:5126 (1993) 1286–1292.

[40] S. Mann, B. R. Heywood, S. Rajam, and J. D. Birchall, "Controlled Crystallization of $CaCO_3$ Under Stearic Acid Monolayers," Nature, 334 (1988), 692–695.

[41] S. Mann and G. A. Ozin, "Synthesis of Inorganic Materials with Complex Form," Nature, 382:6589 (1996), 313–318.

[42] S. Mann, J. Webb and R. J. P. Williams (eds.), Biomineralization: Chemical and Biological Perspectives, VCH, Weinheim, Ger., 1989.

[43] C. B. Murray, C. R. Kagan, and M. G. Bawendi, "Self-Organization of Cdse Nanocrystallites into 3-Dimensional Quantum-Dot Superlattices," Science, 270:5240 (1995), 1335–1338.

[44] R. G. Nuzzo, L. H. Dubois, and D. L. Allara, "Fundamental Studies of Microscopic Wetting on Organic Surfaces. 1. Formation and Structural Characterization of a Self-Consistent Series of Polyfunctional Organic Monolayers," J. Am. Chem. Soc., 112: (1990), 558–569.

[45] S. I. Stupp and P. V. Braun, "Molecular Manipulation of Microstructures: Biomaterials, Ceramics, and Semiconductors," Science, 277:5330 (1997), 1242–1248.

[46] H. H. Teng, P. M. Dove, C. A. Orme, and J. J. De Yoreo, "Thermodynamics of Calcite Growth: Baseline for Understanding Biomineral Formation," Science, 282:5389 (1998), 724–727.

[47] A. Ulman, An Introduction to Ultrathin Organic Films: From Langmuir-Blodgett to Self-Assembly, Academic Press, San Diego, CA., 1991.

[48] D. Walsh, J. D. Hopwood, and S. Mann, "Crystal Tectonics—Construction of Reticulated Calcium-Phosphate Frameworks in Bicontinuous Reverse Microemulsions," Science, 264:5165 (1994), 1576–1578.

[49] J. A. Zasadzinski, R. Viswanathan, L. Madsen, J. Garnaes, and D. K. Schwartz, "Langmuir-Blodgett-Films," Science, 263:5154 (1994), 1726–1733.

[50] X. K. Zhao and J. H. Fendler, "Size Quantization in Semiconductor Particulate Films," J. Phys. Chem., 95: 9 (1991), 3716–3723.

[51] B. J. J. Zelinsky, C. J. Brinker, D. E. Clark, and D. R. Ulrich (eds.), Better Ceramics Through Chemistry, Mat. Res. Soc., Pittsburgh, PA, 1990.

JOANNA AIZENBERG is a member of technical staff in the Materials Research Department, Physical Sciences, at Bell Labs in Murray Hill, New Jersey. She received a B.S. degree in chemistry and an M.S. degree (with honors) in physical chemistry from Moscow State University in Russia and a Ph.D. degree (with honors) in structural biology from the Weizmann Institute of Science in Rehovot, Israel. She joined Bell Labs after a postdoctoral appointment at Harvard University. She currently pursues a broad range of research interests that include biomimetics, nanofabrication, biomineralization, bio-optical materials, biological structural materials, self-assembly, and crystal engineering. One of the pioneers of the rapidly developing field of biomaterials, she is particularly interested in materials properties of natural hybrid organic/inorganic systems, which display "high-tech" properties, and the lessons that industry can borrow from them. With 10 patents and more than 50 papers to her credit, Dr. Aizenberg has won a number of awards for her research, including the Max-Planck Society award in the field of biology and materials science, Germany (1995); the Arthur K. Doolittle Award, ACS (1999); the New Investigator Award in Chemistry and Biology of Mineralized Tissues (2001); and the ACS PROGRESS Lectureship Award (2004). ◆